Muscle Synergy Organization Is Robust Across a Variety of Postural Perturbations

Gelsy Torres-Oviedo, Jane M. Macpherson and Lena H. Ting

You might find this additional information useful...

This article cites 55 articles, 38 of which you can access free at:
http://jn.physiology.org/cgi/content/full/96/3/1530#BIBL

Updated information and services including high-resolution figures, can be found at:
http://jn.physiology.org/cgi/content/full/96/3/1530

Additional material and information about *Journal of Neurophysiology* can be found at:
http://www.the-aps.org/publications/jn

This information is current as of August 19, 2006 .

Muscle Synergy Organization Is Robust Across a Variety of Postural Perturbations

Gelsy Torres-Oviedo,[1] **Jane M. Macpherson,**[2] **and Lena H. Ting**[1]
[1]*The Wallace H. Coulter Department of Biomedical Engineering, at Georgia Tech and Emory University, Atlanta, Georgia; and*
[2]*Neurological Sciences Institute, Oregon Health and Sciences University, Beaverton, Oregon*

Torres-Oviedo, Gelsy, Jane M. Macpherson, and Lena H. Ting.
Muscle synergy organization is robust across a variety of postural
perturbations. *J Neurophysiol* 96: 1530–1546, 2006. First published
June 14, 2006; doi:10.1152/jn.00810.2005. We recently showed that
four muscle synergies can reproduce multiple muscle activation pat-
terns in cats during postural responses to support surface translations.
We now test the robustness of *functional* muscle synergies, which
specify muscle groupings and the active force vectors produced
during postural responses under several biomechanically distinct con-
ditions. We aimed to determine whether such synergies represent a
generalized control strategy for postural control or if they are merely
specific to each postural task. Postural responses to multidirectional
translations at different fore-hind paw distances and to multidirec-
tional rotations at the preferred stance distance were analyzed. Five
synergies were required to adequately reconstruct responses to trans-
lation at the preferred stance distance—four were similar to our
previous analysis of translation, whereas the fifth accounted for the
newly added background activity during quiet stance. These five
control synergies could account for >80% total variability or $r^2 > 0.6$
of the electromyographic and force tuning curves for all other exper-
imental conditions. Forces were successfully reconstructed but only
when they were referenced to a coordinate system that rotated with the
limb axis as stance distance changed. Finally, most of the functional
muscle synergies were similar across all of the six cats in terms of
muscle synergy number, synergy activation patterns, and synergy
force vectors. The robustness of synergy organization across pertur-
bation types, postures, and animals suggests that muscle synergies
controlling task-variables are a general construct used by the CNS for
balance control.

INTRODUCTION

Recent findings suggest that the CNS simplifies motor con-
trol by constraining muscles to be activated in fixed groups, or
synergies, where each synergy is defined as a set of muscles
recruited by a single neural command signal. Complex muscle
activation patterns in a wide range of motor tasks including
locomotion, finger spelling, and postural tasks, can be decom-
posed into the summed activation of just a few muscle syner-
gies (d'Avella and Bizzi 2005; d'Avella et al. 2003; Ivanenko
et al. 2003, 2004; Krishnamoorthy et al. 2003; Poppele and
Bosco 2003; Poppele et al. 2002; Ting and Macpherson 2005;
Tresch et al. 1999; Weiss and Flanders 2004). A muscle
synergy control structure provides an attractive simplifying
strategy for the control of complex movements because it
reduces the number of output patterns that the nervous system

must specify for a large number of muscles yet allows flexi-
bility in the final expression of muscle activation.

A synergy control structure not only simplifies the motor
output pattern for muscle activation but may also be function-
ally related to high-level control parameters—global biome-
chanical variables that are important for movement control. For
example, Ting and Macpherson (2005) demonstrated in cats
that four muscle synergies could account for the spatial tuning
patterns of the automatic postural response elicited by support
surface translations in multiple directions in the horizontal
plane. These synergies appear to specify the appropriate end-
point forces at the ground that are required to maintain balance
(Ting and Macpherson 2005). Muscle synergy recruitment has
also been correlated to center of mass shifts in standing
(Krishnamoorthy et al. 2003), foot and limb kinematics in
walking (Ivanenko et al. 2003, 2004), foot acceleration in
pedaling (Ting et al. 1999), and hand kinematics in finger
spelling (Weiss and Flanders 2004). Muscle synergies may
therefore reflect a neural control strategy at the level of func-
tional variables specific to the particular motor task at hand.

For a muscle synergy structure to be useful in reducing the
degrees of freedom to be controlled during movement, the
observed synergies must be limited in number and robust
across behavioral tasks and subjects. Only a few studies have
directly examined these features of robustness and generality.
Studies in frogs demonstrate synergies that are shared for
walking, jumping, and swimming and those that are unique to
each locomotor mode (d'Avella and Bizzi 2005). In addition,
simulations and experiments in human pedaling show that the
same functional muscle groups can be used to perform varia-
tions within the task such as fast or slow, smooth or jerky,
forward, backward, or one-legged pedaling (Raasch and Zajac
1999; Raasch et al. 1997; Ting et al. 1998–2000). On the other
hand, Krishnamoorty et al. (2004) showed that postural syner-
gies are specific to the task since they change with changes in
stability conditions during standing, and new muscle synergies
(M-modes) emerge to account for changes in the postural
responses.

The current study explicitly addresses both robustness and
generality by examining the extent to which muscle synergies
and their biomechanical functions described for postural re-
sponses in the cat (Ting and Macpherson 2005) generalize
across tasks and subjects. We chose to modify the conditions
under which postural responses were elicited in two ways:
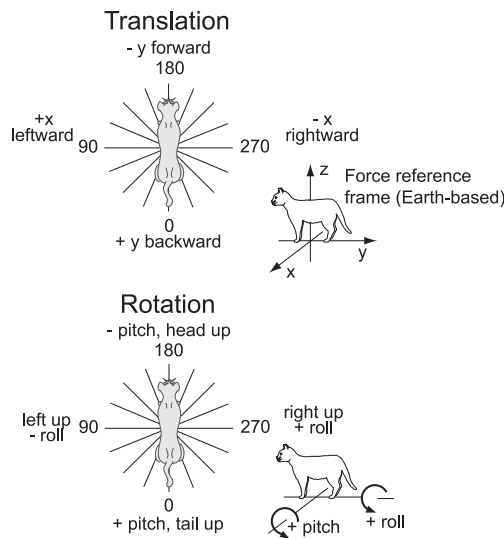altering the configuration of the limbs during support surface

---

FIG. 1. Coordinate system for support surface translations and rotations in 16 evenly spaced directions around the horizontal plane. The coordinate systems used to describe rotation and translation directions were defined such that the horizontal displacement of the cat's center of mass (CoM) relative to the feet was in the same direction at the end of each translation or rotation. For example, a backward platform translation and a head down rotation are defined as perturbations in same 0° direction because both displace the cat's CoM forward, relative to the feet. The coordinate system of force plate recordings is also shown.

translations by varying the stance distance between the fore- and hind-paws and changing the perturbation characteristics such that the support surface was rotated in combinations of pitch and roll rather than horizontal plane translations.

Because these experimental manipulations induce variability in the automatic postural response, the tolerance of synergies to this variability is a reasonable test of their robustness. First, in both humans and cats, changing the stance distance has been shown to modify the forces and electromyograms (EMGs) produced during postural responses and quiet stance (Fung and Macpherson 1999; Henry et al. 2001; Macpherson 1994). In particular, the force responses in the horizontal plane change from being constrained to two directions (force constraint strategy) at long stance distances to a more uniform distribution at short distances (Henry et al. 2001; Macpherson 1994). Second, translations and rotations of the support surface produce similar EMG responses in extensors but not flexors (Ting and Macpherson 2004). Moreover, extensor responses during rotations and translations are elicited during disparate kinetic and kinematic conditions. For example, extensors are activated when the hindlimb is initially loaded in translations but also when it is unloaded in rotations. Thus the extensors are activated when joint angles undergo flexion in translation versus extension in rotation, and the extensors are stretched in translation versus shortened in rotation.

We hypothesized that the synergy organization for postural control is robust such that a single set of functional muscle synergies underlies a variety of automatic postural responses under differing conditions. Our results show that for all limb postures and perturbation types, the same set of muscle synergies and endpoint force vectors could reproduce the entire range of muscle and force responses observed during quiet stance and during multidirectional balance perturbations. We also hypothesized that the synergy organization is generalized

across subjects. Our results show considerable similarity in both synergy composition and endpoint force across animals. Our findings of robustness and generality suggest that muscle synergies controlling endpoint forces represent a general control structure used for maintaining balance, independent of the particular postural conditions.

METHODS

Experimental setup

To investigate the effect of limb configuration and perturbation type on muscle synergies used during postural control in the cat, we analyzed previously collected postural responses to multidirectional support surface translations at different fore-hindlimb stance distances (Macpherson 1994) and multidirectional platform rotations and translations (Ting and Macpherson 2004). Functional muscle synergies were extracted from the control condition of multidirectional translation at the preferred stance distance and used to reconstruct all of the other test conditions. Detailed experimental and training procedures were described previously (Macpherson et al. 1987). A brief overview of the experimental setup and data collection procedures is presented here.

Cats were trained to stand freely with one foot on each of four triaxial force plates. Each plate was mounted on the perturbation platform using a magnet and double-sided tape, thus allowing the position of each plate to be easily manipulated between experimental sessions to effect a change in stance distance. Translation perturbations consisted of ramp-and-hold displacements of 5-cm amplitude, 370-ms duration, and 15-cm/s mean peak velocity in 12 or 16 directions evenly spaced in the horizontal plane. Rotation perturbations consisted of ramp-and-hold platform tilts in 16 combinations of pitch and roll of 6° amplitude, 200-ms duration and 40°/s mean peak velocity. Platform rotation amplitude was chosen to produce similar rotation about the metacarpophalangeal (MCP) and metatarsophalangeal (MTP) joints as was observed during translation. The coordinate systems used to describe rotation and translation directions were defined such that the direction of the horizontal displacement of the cat's center of mass (CoM) relative to the feet was the same at the end of each translation or rotation (Fig. 1).

After training was completed, muscles in each cat were implanted with indwelling bipolar wire electrodes (Teflon-coated multi-stranded stainless steel, Cooner AS632) under general anesthesia using aseptic technique (see Macpherson 1988b). Electrode wires were accessed through two connectors mounted on the cat's head. EMG activity was recorded from a subset of 8–15 left hindlimb muscles in each of six cats. Table 1 contains an inclusive list of all the recorded muscles. Cats were allowed to recover fully from the surgery before participating in experiments.

TABLE 1. *Inclusive list of the muscles recorded from the left hindlimb across cats*

Label	Muscle Name	Label	Muscle Name
GLUT	Gluteus medius		
GLUP	Posterior gluteus medius	SRTM	Medial sartorius
GLUA	Anterior gluteus medius	STEN	Semitendinosus
VLAT	Vastus lateralis	BFMA	Anterior biceps femoris
VMED	Vastus medialis	BFMM	Medial biceps femoris
SOL	Soleus	BFMP	Posterior biceps femoris
PLAN	Plantaris	REFM	Rectus femoris
EDL	Extensor digitorum longus	SEMA	Anterior semimembranosus
ILPS	Iliopsoas	SEMP	Posterior semimembranosus
TFL	Tensor fasciae latae	GRAA	Anterior gracilis
FDL	Flexor digitorum longus	GRAP	Posterior gracilis
TIBA	Tibialis anterior	MGAS	Medial gastrocnemius
SRTA	Anterior sartorius	LGAS	Lateral gastrocnemius

Three recording sessions for each experimental condition were performed on separate days. For three cats, postural responses to translations were measured when cats were standing at three or four different inter-paw distances. The anterior-posterior (AP) distance between the fore-and-hind paws was varied from 48 to 138% of the preferred distance of each cat. The preferred distance was defined as the fore-hind paw separation assumed by an individual cat while standing unrestrained on the lab floor. For a given stance distance, five trials were collected at each of 12 evenly spaced perturbation directions. Kinematic data from body segments were collected at 100 Hz using an Optotrak (Northern Digital, Waterloo, Ontario, Canada) system. For three other cats, postural responses to 16 directions of translation and rotation at the preferred stance distance were recorded (5 trials per direction). Ground reaction forces (GRF) and EMGs were collected at 1,000 Hz for translation and 1,200 Hz for rotation, using an Amlab system (Amlab Technologies, Lewisham, NSW, Australia). Kinematic data from body segments were collected at 120 Hz using a Vicon system (Vicon, Lake Forest, CA). Data were filtered and processed off-line using a set of custom MATLAB routines. Forces were low-pass filtered at 100 Hz, and EMG data were high-pass filtered at 35 Hz, de-meaned, rectified, and then low-pass filtered at 30 Hz.

Data processing

In summary, for each perturbation direction, we generated data vectors consisting of the mean EMG activity and forces generated during a background period (BK) and during the automatic postural response (APR). Thus each experimental condition was characterized by a matrix of data where the rows represent muscles and forces and the columns represent their activity during background and APR period for each perturbation direction.

To obtain the mean EMG and force data for the data matrix, the first step was to average trials by perturbation direction within each session. From each set of averages, the EMG background (EMG_{BK}) was computed as the mean EMG during a 200-ms window that ended 50 ms prior to perturbation onset. Similarly, the EMG of the postural response (EMG_{APR}) was computed as the mean EMG during an 80-ms window beginning 60 ms after perturbation onset (Macpherson 1988b) (Fig. 2). EMG_{APR} amplitude varies as a function of perturbation direction and represents the muscle tuning curve (e.g., Fig. 6). Background forces (F_{BK}) during quiet stance were computed as the mean ground reaction force under the left hindlimb in the same period as EMG_{BK}. The active force during the postural response (F_{APR}) was computed as the change in force from background levels during an 80-ms window that began 60 ms after EMG_{APR} onset or 120 ms after perturbation onset (Jacobs and Macpherson 1996) to accommodate excitation-contraction coupling time. This definition of active force was used in our previous work in which only *change* in force from background was related to EMG (Jacobs and Macpherson 1996; Macpherson 1988a,b; Ting and Macpherson 2005).

We separated out the positive and negative components of the forces (*x, y,* and *z*) to match the functional characteristics of muscle in that muscles and muscle synergies can produce forces, in only one direction along an axis. The generation of force in positive and negative directions is accomplished by different synergies as demonstrated by our previous studies (Jacobs and Macpherson 1996; Macpherson 1988b; Ting and Macpherson 2005). Thus the F_{BK} during quiet stance was expressed as six values corresponding to absolute values of the positive and negative directions of the force vector components (F_{BKx+}, F_{BKx-}, F_{BKy+}, F_{BKy-}, and F_{BKz+}, F_{BKz-}). The F_{APR} of the postural response was expressed as six values corresponding to the absolute values of the positive and negative *change* in force from background levels (F_{APRx+}, F_{APRx-}, F_{APRy+}, F_{APRy-}, and F_{APRz+}, F_{APRz-}; Fig. 3). Expressing the force components as absolute values was a requirement of the nonnegative analysis method that we chose (see *Extraction of functional muscle synergies*).
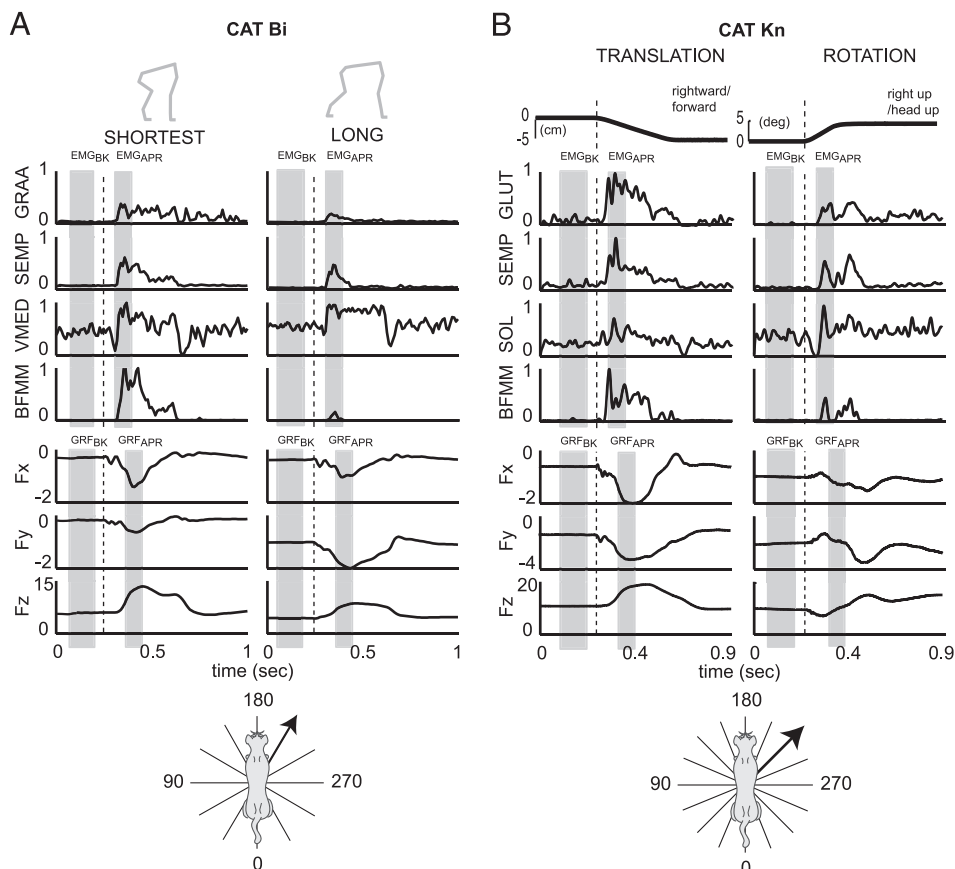

FIG. 2. Left hindlimb EMG and force responses of 2 cats during different experimental conditions. *A*: responses of *cat Bi* to 210° platform translation at shortest (13 cm) and long (34 cm) stance distances. Overall, the electromyographic (EMG) activity of most of the recorded muscles was higher at short stance compared with long. *B*: responses of *cat Kn* to 225° translation and rotation. Note the overall smaller amplitude of response for rotation compared with translation. Vertical dashed lines mark onset of platform motion. In all cats, the EMG_{BK} and GRF_{BK} responses during background, were quantified by the mean activity over the shaded area before platform onset. Similarly, EMG_{APR} and GRF_{APR} were quantified by the mean activity over the time window indicated by the shaded areas following platform onset. Note the time offset between the EMG_{APR} period and the GRF_{APR} period. Passive changes in force due to platform motion are observed between the dashed line and the gray area indicating the GRF_{APR} window. In the case of platform rotation, note that passive changes in force are relatively large and in the opposite direction to changes in force during the GRF_{APR} window.
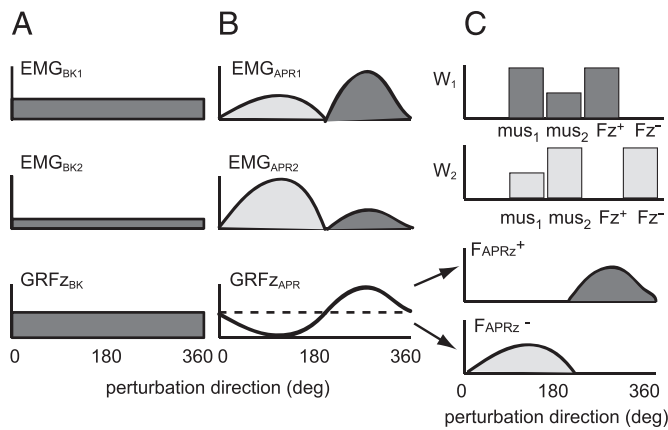
FIG. 3. Schematic diagram of EMG and force analysis procedure. *A*: example of background EMG from 2 muscles, EMG_{BK}, and vertical force, $GRFz_{BK}$ during quiet stance prior to each perturbation direction. *B*: example tuning curves for the postural response, EMG_{APR}, of the 2 muscles, and force tuning curve for the vertical component during the postural response, $GRFz_{APR}$. In this example, the 2 muscles are co-activated at each direction while $GRFz_{APR}$ decreases below background levels for directions 0–180° and increases for 180–360°. *C*: W_1 and W_2 represent functional muscle synergies extracted from the example data. Both muscles (mus_1 and mus_2) are active in each synergy but with different relative levels of activation (dark and light shaded areas under the EMG tuning curves in *B* correspond to the activation of synergies 1 and 2, respectively). Before synergy extraction, the active force is decomposed into the absolute values of positive and negative changes from background levels (*bottom 2 plots*). Synergy 1 is associated with a change in the positive *z* force (F_{APRz+}) and synergy 2, with the negative *z* force (F_{APRz-}).

The treatment of APR forces from rotation trials was slightly different from that of translation. Unlike translations, rotations cause large changes in passive force between the onset of the platform motion and the APR, primarily due to the projection of the weight-support force (F_z) into the *x-y* plane of the force plates as the platform tilts (Ting and Macpherson 2004). Thus the change in force of the APR was computed with respect to the passive force level and not the background force. The maximum passive force was defined as the peak force level (in platform-based coordinates) (Ting and Macpherson 2004) that occurred at 80 ms after perturbation onset. The passive forces in translations (observed only in the *x* and *y* components) are small (<5% of the F_{APR} amplitude) and dominated by the motion artifact due to the platform acceleration. Because of the small amplitude and the difficulty in accurately estimating the passive force in translation, we did not subtract passive forces from the F_{APR} in translations.

In summary, for each experimental condition, the data pool consisted of a vector for each muscle in which the elements represented EMG_{BK} and EMG_{APR} across perturbation directions and a vector for each of the six force components in which the elements represented F_{BK} and F_{APR} for each perturbation direction. For display and data inspection prior to synergy analysis, EMGs and forces were normalized to their respective maximum response amplitude across all experimental conditions so that all values were between 0 and 1. Then each data vector consisting of either an EMG signal or a force component was normalized to have unit variance in the control condition, which allowed the different data types to be combined. EMG and force data from the test conditions were normalized with the same factors as the control condition to maintain consistent units across conditions.

Extraction of functional muscle synergies

The matrix for extracting functional muscle synergies consisted of both muscle [EMG_{BK}, EMG_{APR}] and force data [F_{BK}, F_{APR}]. Therefore a functional muscle synergy consists of pairs of covarying

patterns of muscle activation (muscle synergies, W_{EMG}) and force generation (synergy force vectors, W_F) and each muscle synergy is assumed to have the function of generating a synergy force vector. This approach differs from our previous study, in which muscle synergies and endpoint forces were extracted separately and then correlated (Ting and Macpherson 2005).

By extracting synergies conjointly from muscle and force data, we tested the hypothesis that the force data could be reconstructed using a set of force vectors whose magnitudes scale with the activation of muscle synergies. While the synergy force vectors represent the forces most likely to be generated by muscle synergy activation, they may not be orthogonal or independent vectors and may not span the entire force space. The conjoint method has the further effect of ignoring components of force not directly generated by muscle activation in the limb, such as those due to dynamic or inertial forces or to forces generated by muscles in a different limb.

Because the main purpose of this study was to explore dimensionality of the muscle activations and the robustness of muscle synergy composition, we tested whether the presence of force data in the data matrix influenced the composition of the resultant muscle synergy vectors. Synergies extracted from the EMG data both with and without the force data showed the same dimensionality (5) and very similar muscle composition ($r^2 > 0.9$ for all synergies across all cats). Therefore addition of the forces to the data set changed neither the dimensionality of the synergies nor their composition.

We used a linear decomposition technique called nonnegative matrix factorization (NMF) to extract functional muscle synergies (Lee and Seung 2001). This formulation is mathematically identical to that presented in both Tresch et al. (1999) and Ting and Macpherson (2005) but uses a more efficient algorithm. For each perturbation direction k, the vector X_k represents a concatenation of all of the muscle and force responses during quiet stance or during the APR period. Thus 32 data vectors, X_k, were generated from 16 perturbation directions (16 BK and 16 APR vectors). A functional muscle synergy is represented as a vector W_n formed by a group of muscles and the endpoint force generated by their activation. The data vectors, X_k, for each given perturbation direction, k, can be reconstructed using a weighted sum of functional muscle synergy vectors

$$X_k \cong \sum_{n=1}^{Nsyn} c_{nk} W_n$$

where X_k = [$EMG_{BK} F_{BK}$]$_k$ or [$EMG_{APR} F_{APR}$]$_k$, c_{nk} is a nonnegative coefficient representing the activation level of synergy n in direction k, and W_n is composed of muscle and force individual gains (w_{ni} and f_{nj}) that specify the activation level of each muscle, i, within the synergy and of each component, j, of the synergy force vector for each functional synergy. All the elements of each functional synergy are constrained to be positive and constant over all conditions. For each synergy n, the set of activations c_{nk} across all perturbation directions during quiet stance and during the APR period is the vector C_n. The C_n components during the APR period represent the tuning curve that describes how the activation of the functional muscle synergy W_n changes as a function of perturbation direction.

The number of functional muscle synergies that best characterized the data were determined by one global criterion and two local criteria: total percentage variability accounted for (VAF) >90% in the control condition, a roughly uniform distribution of errors as a function of perturbation direction within each condition as determined by evaluating the effect of adding an additional synergy, and adequate reconstruction of each muscle tuning curve for each perturbation direction in all conditions, as determined by either $r^2 > 0.6$ or VAF >80%.

VAF is defined as 100* uncentered Pearson correlation coefficient, which requires the regression to pass through the origin (Zar 1999). This is a similarity metric that is used to quantify exact matches between two patterns such as genomic sequences (Alizadeh et al.

2000; Eisen et al. 1998). The definition of both r^2 and VAF is $(1 - \text{sum of squared errors/total sum of squares})$. However, in the standard Pearson correlation coefficient (r^2), the total sum of squares is taken with respect the mean value of y, whereas in the uncentered case (VAF), it is taken with respect to zero.

VAF is a more stringent criterion than r^2 because it evaluates both shape and magnitude of the measured and reconstructed curves. VAF is equal to 100% when the two curves are perfectly matched, that is, the regression between them has a slope of 1 and offset of 0. r^2 is only sensitive to the similarity in shape of the curves without constraining the slope or offset of the regression. r^2 provided a better assessment of the reconstruction in the case where the tuning curve shapes were well-matched, but the amplitude was not, whereas VAF was higher for muscles with high baseline activity and noisy tuning curves (e.g., LGAS in Fig. 9). If a muscle tuning curve was flat (i.e., muscle activation was constant across direction), the r^2 and VAF values from that muscle were not included in the criteria for selecting the number of functional muscle synergies because such muscles were not selectively activated during postural responses.

The combination of both global and local variability criteria ensured that each pattern of muscle activation measured for a given perturbation direction, and each muscle tuning curve over all directions was well-reconstructed. This allowed identification of functional muscle synergies that may account for only a small percentage of the total data variability but are essential to reproduce the responses to a specific range of perturbation directions (Ting and Macpherson 2005).

Data analysis

Functional muscle synergies (W) were first extracted from the control data set of multidirectional translations at the preferred stance distance. These control synergies were then tested for robustness within subjects by using them to reconstruct the test data from translations at nonpreferred stance distances and rotation perturbations. Finally, synergy vectors were compared across cats to test the generality of the synergy structure across individuals.

In the first test, functional muscle synergies extracted from control data were used to reconstruct EMG and force responses to platform translation at all stance distances by performing a nonnegative least-square fit. Using custom MATLAB routines, we determined the coefficients C_{shortest}, C_{short}, $C_{\text{preferred}}$, and C_{long} that would best reconstruct the translation data at each distance using the control synergies.

In the second test, functional muscle synergies extracted from the control data of translations were used to reproduce EMG and force responses to platform rotations. The reverse procedure of using the rotation synergies to reconstruct the translation responses was not done because rotation does not activate the full muscle set, with the most notable absence being the flexors (Ting and Macpherson 2004). Therefore flexor responses to translation perturbations could not be reconstructed using rotation synergies extracted from data where flexor responses are smaller or nonexistent. Similar to the stance distances analysis, a nonnegative least squares fit of the translation vectors to the rotation data set was performed to find the coefficients C_{rotn} that would best reconstruct the rotation data.

To test the generality of synergy structure, the features of the synergies were compared across cats that followed the same experimental paradigm. Functional synergy vectors (W), muscle synergies (W_{EMG}), synergy force vectors (W_F), and synergy activation coefficients (C) were compared by calculating the coefficients of determination between cats. The muscles that were not common to all the cats were excluded from the muscle synergy vectors before correlation analysis.

RESULTS

For each cat, a set of five functional muscle synergies extracted from the control data was found to account for the muscle activation patterns associated with quiet stance and with the automatic postural response for all five test conditions: multidirectional support surface translations at four nonpreferred stance distances and multidirectional rotations. When muscle activation in a test condition varied from the control condition, this was achieved by changes in the directional tuning of the activation coefficients for the various synergies with some synergies varying more than others. Each functional muscle synergy was characterized by a unique synergy force vector. Forces recorded in the test conditions were well-reconstructed from the control synergy force vectors but only when the force data were referenced to a coordinate system that rotated with the hindlimb axis (defined by the vector from the MTP to hip joints). In other words, the net direction of force produced in space by each muscle synergy rotated with the limb axis. Finally, all animals exhibited similar functional muscle synergies in terms of muscular patterns, force direction, and activation.

Five synergies extracted from preferred stance reproduce responses at all stance distances

A minimum of five functional muscle synergies extracted from the control condition was found to reproduce muscle activation patterns and forces over all perturbation conditions within the specified parameters of acceptability. As the specified number of control synergies was increased from one to eight, the reconstruction of both control and test conditions also increased (Fig. 4A). Across the three cats in the stance distance group, five synergies accounted for a total mean VAF of $96.6 \pm 0.8\%$ in the control dataset at the preferred distance. The total mean VAF accounted for in the test dataset was $84.6 \pm 8\%$ (shortest), $89.7 \pm 3.5\%$ (short), and $79.6 \pm 9.8\%$ (long). The fore-hindpaw stance distances from *cat Bi,* the data of which are illustrated in this section, were 13 cm (shortest), 20 cm (short), 27 cm (preferred), and 34 cm (long). Three functional muscle synergies reproduced 90% of the overall data variability in *Bi* at the preferred stance (Fig. 4A), but not all directions were adequately reconstructed (Fig. 4B). Adding the fourth and fifth synergy dramatically improved the directional profile of VAF, particularly at 0 and 150°. For example, when the synergy number was increased from 4 to 5, the VAF for the 150° perturbation direction at the shortest stance distance increased from $\sim$60 to $> 80\%$ in cat Bi (Fig. 4B, preferred to shortest). Five synergies from the preferred stance dataset were also required to reconstruct all EMG tuning curves to $r^2 > 0.6$ (Table 2). The only EMG tuning curve excluded from the analysis was from *cat Ru* at long stance where SRTM was inactive. A minimum of five synergies was needed to adequately reconstruct the EMG responses across all directions as well as quiet stance. For more than five, the added synergies contributed about evenly to the reconstruction of responses across all perturbation directions, suggesting that the extra synergies represented random variations in the data.

The inclusion of the force data in the synergy analysis did not alter the muscle composition of each synergy or the number of muscle synergies required to adequately reconstruct the EMG data (Fig. 4C). Therefore the dimension and composition of the functional synergies primarily reflects variability within the muscle activation pattern, and not the forces.
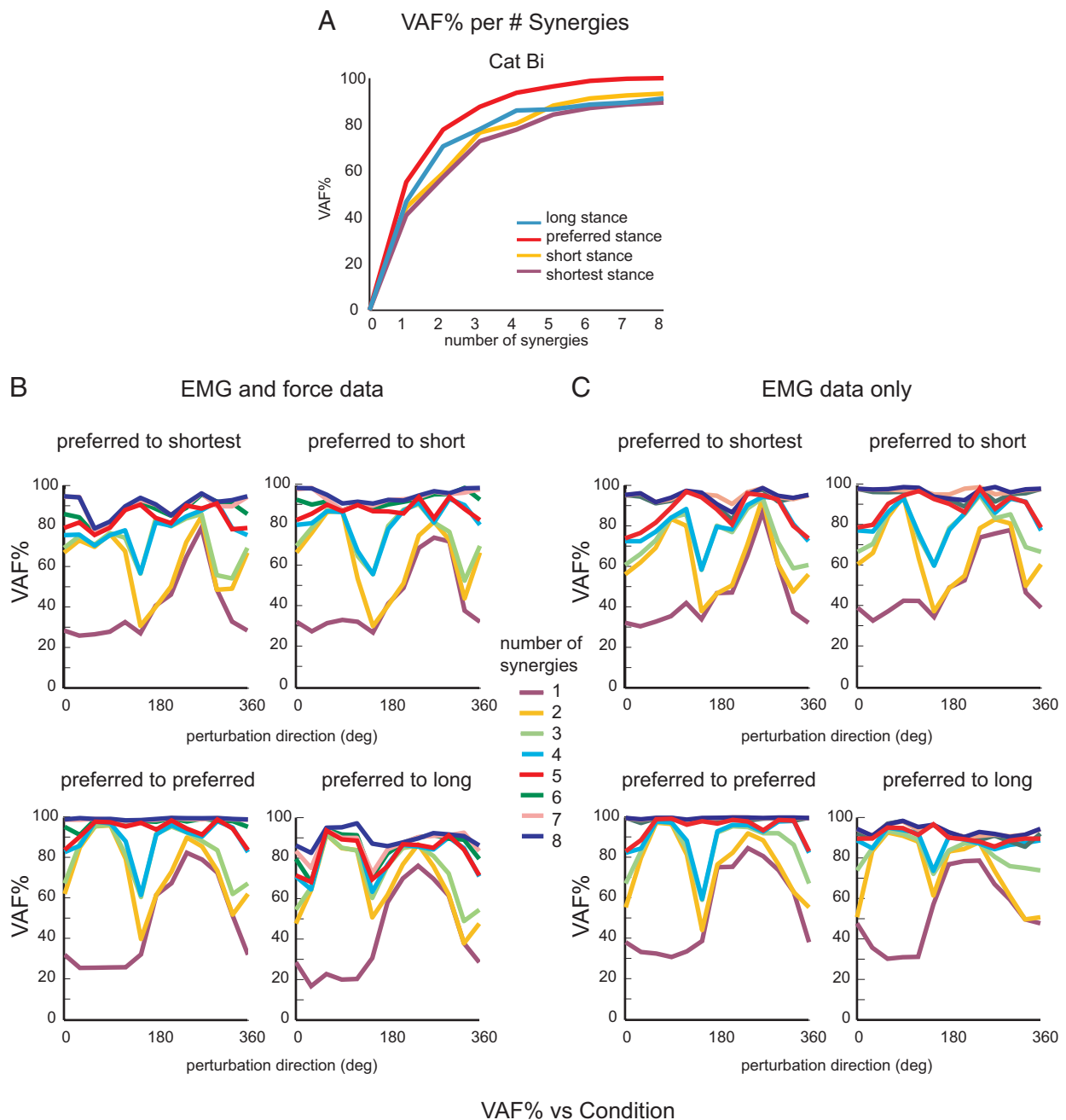
FIG. 4. *A*: variability accounted for by increasing numbers of synergies for entire datasets at each stance distance for *cat Bi*. Five synergies accounted for 96% of total variability in translation at the preferred stance (red line). These same 5 synergies accounted for 84, 88, and 87% of the total data variability at shortest, short, and long stance, respectively. *B*: variability accounted for at each stance distance as a function of perturbation direction for *cat Bi*. The synergies used to obtain these VAF values were extracted from EMG and force responses during background and APR periods. *C*: variability accounted for at each stance distance of *cat Bi* when synergies were extracted from EMG data only. The dimensionality of the synergy set used to characterize muscle postural responses was the same whether or not forces were included in the synergy extraction analysis.

Each synergy, W_n, was reasonably distinct in terms of muscle composition (Fig. 5*A*) and directional tuning of the activation coefficients, C_n, (Fig. 5*B*) (cf. Ting and Macpherson 2005). Only one synergy, W_1 was active during the background period to provide antigravity support and consisted primarily of the vasti muscles in *cat Bi* (Fig. 5, red synergy). During the APR, the activity of W_1 was decreased from that of quiet stance for perturbations between 210 and 300° when the left hindlimb was loaded (increased vertical force) and shut down completely for all other directions. W_2 (Fig. 5, yellow synergy) was

active from 330 to 120°, when the left hindlimb was unloaded, and contained the uniarticular hip flexor iliopsoas, as well as biarticular muscles with a knee flexion moment arm such as sartorius, semitendinosus, and posterior biceps femoris. The composition of W_3 (Fig. 5, green synergy) included many hip extensors, such as anterior and posterior gluteus, vastus medialis and lateralis, middle biceps femoris, posterior semimembranosus, and gracilis. W_4 (Fig. 5, blue synergy) was dominated by rectus femoris, a hip flexor, and knee extensor with activity from the synergist, anterior sartorius, hip extensors

TABLE 2. *r^2 values of EMG and force tuning curve reconstructions in the stance distance group*

Cat	r^2 Shortest			r^2 Short			r^2 Preferred			r^2 Long		
	Minimum	Maximum	Average	Minimum	Maximum	Average	Minimum	Maximum	Average	Minimum	Maximum	Average
Summary of electromyographic (EMG) reconstruction												
Ru	0.69	0.98	0.90	0.73	0.99	0.93	0.88	1.00	0.96	0.61	0.99	0.88
Bi	0.63	0.98	0.86	0.73	0.99	0.87	0.88	0.99	0.94	0.73	0.95	0.88
Ni	0.57	0.98	0.88	0.81	0.99	0.91	0.81	1.00	0.94	na	na	na
Summary of Force reconstruction												
Ru	0.74	0.95	0.84	0.59	0.96	0.82	0.56	0.96	0.85	0.60	0.92	0.77
Bi	0.55	0.96	0.79	0.59	0.98	0.81	0.81	0.99	0.90	0.75	0.97	0.88
Ni	0.74	0.96	0.88	0.84	0.96	0.90	0.87	0.98	0.91	na	na	na

vastus lateralis and medialis and moderate activity from the uniarticular hip flexor iliopsoas; it's tuning curve overlapped with that of the flexors in W_2 but was phase-shifted to the right. W_5 (Fig. 5, purple synergy) was dominated by the hamstring muscles and especially gracilis, and its activation overlapped with the flexors in W_2 but with a phase-shift to the right.

Activation of functional muscle synergies changes with stance distance

All five control synergies contributed to translation postural responses at all stance distances, however the activation level of some synergies decreased as stance distance increased (Fig. 5B). W_3 and W_5, formed largely by biarticular muscles, varied the most in activation across stance distance. The peak activations in W_3 and W_5 at the longest stance were 32.5 and 13% of their respective peak activations at the shortest stance. W_4 and W_2, the flexor-dominated synergy, were less modulated with distance (peak at the long stance was 74.5 and 59.4% of their respective peak activations at the shortest stance). Activation of W_1 during the background period and the postural responses was little affected by stance distance. W_5 broadened its activation to include more directions at long stance, W_4 shifted its activation to the right at short and shortest stances, and W_2 and W_3 maintained the same directional tuning with stance.

The EMG tuning curves were adequately reconstructed at all stance distances using the five synergies from the control condition (Fig. 6). Overall, tuning curve shape was well reconstructed for all EMGs, whereas amplitude was less well reconstructed for a subset of muscles. The coefficients of determination (r^2) between the original and the reconstructed data exceeded 0.8 in 97.9% of the muscle tuning curves across all stance distances and all cats while the variance accounted for (VAF) exceeded 96.5% in 80% of the individual muscle tuning curves. In some muscles of *cat Bi* (anterior gracilis, middle biceps femoris, and anterior sartorius), EMG amplitude was greater at the short stances than was predicted by the linear modulation of the muscle synergy (Fig. 6). However, the direction at which peak activation occurred and the tuning curve shapes were well predicted, suggesting that these muscles might still be activated by the same synergies, but with a nonlinear amplitude scaling.

Synergy force vectors are consistent with respect to the limb axis

Each of the five control synergies was characterized by a distinct force vector (W_F; Fig. 5C). Initial attempts to reconstruct GRF responses to platform translation using this control set of synergy W_Fs were successful only at reconstructing data from the preferred stance distance and not from the other distances. We attributed the difficulty in force reconstruction to the large change in GRF vector orientation that accompanies changes in stance distance.

Our previous study showed that during quiet stance, the angle of both the limb axis and the GRF vector changed linearly with stance distance, with the GRF vector angle having a slightly smaller gain than that of limb axis angle (Fung and Macpherson 1995). Therefore we transformed the original force data into the coordinate system of the average GRF vector that was measured during quiet standing at each stance distance, named here the F-frame (Fig. 7, *A* and *B*). Once transformed, acceptable reconstruction of all the force data were achieved at the $r^2 > 0.6$ level (Table 2) using control synergy force vectors, except for Fx- ($r^2 = 0.55$ and $r^2 = 0.59$) of *cat Bi* at the short and shortest stance and Fx- ($r^2 = 0.58$ and $r^2 = 0.56$) of *cat Ru* at the short and preferred stance. This result suggests that synergies produce consistent forces in a limb-referenced coordinate system. As shown in Fig. 7A, the z axis was specified as the mean GRF vector during quiet stance and the x axis was defined to be collinear with the x axis of the Earth coordinate system (a vector pointing laterally). The GRF vector and the hindlimb axis varied mainly in the sagittal plane with stance distance. As a result, the force data in each configuration were rotated about the x axis by an angle θ, defined as the angle between the z axis of the Earth coordinate system and that of the hindlimb GRF coordinate system. When expressed in the hindlimb coordinate system, the anterior-posterior (Fy) forces show consistent phasing relative to perturbation direction across stance distance, unlike the tuning curves of the same Fy forces in the Earth coordinate system (Fig. 7D). The angles of rotation for each stance configuration in all the cats are reported in Table 3.

When viewed in the F-frame coordinate system, the five W_Fs, appear to have a consistent function across all stance distances. In the sagittal plane (Fig. 7A), W_{F1} and W_{F2} were aligned approximately with the limb axis with W_{F1} having a downward, or loading component and W_{F2} an upward compo-

A Muscle Synergies (W_{EMG})
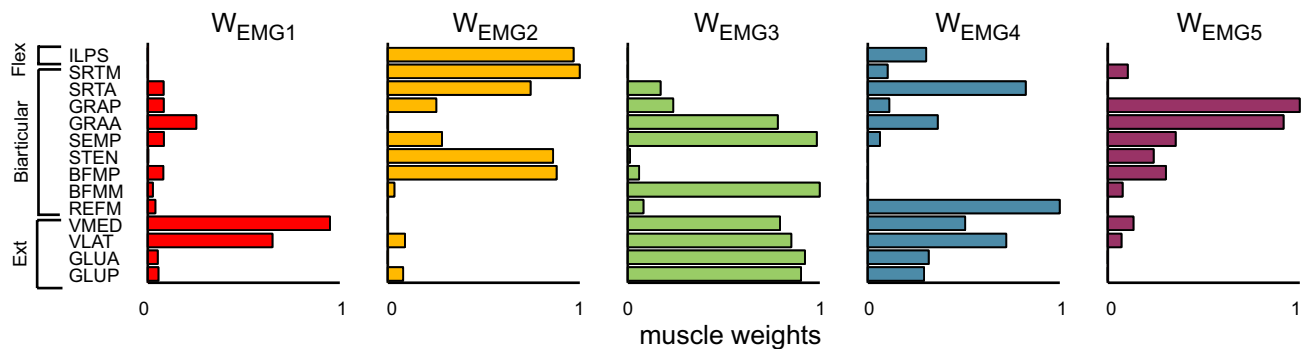
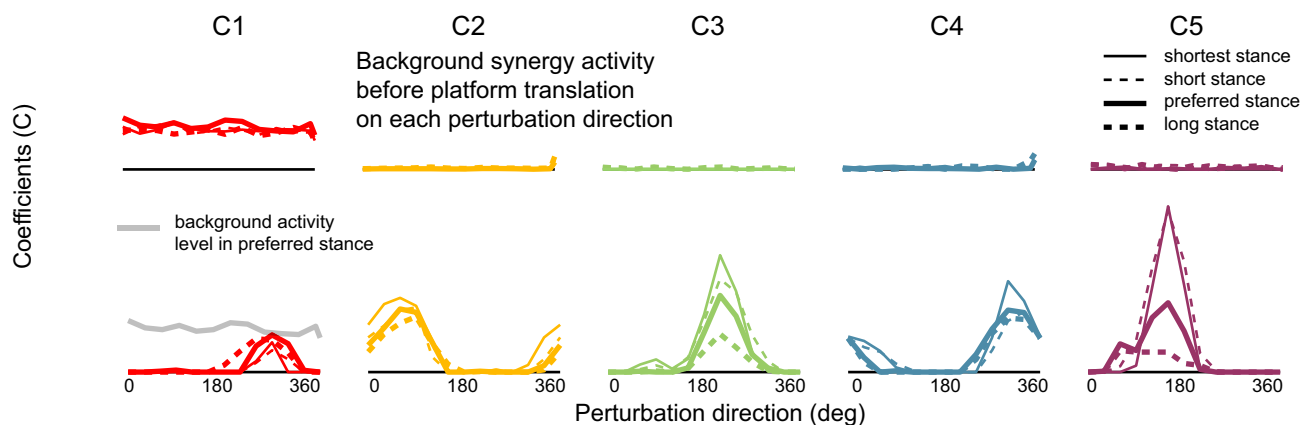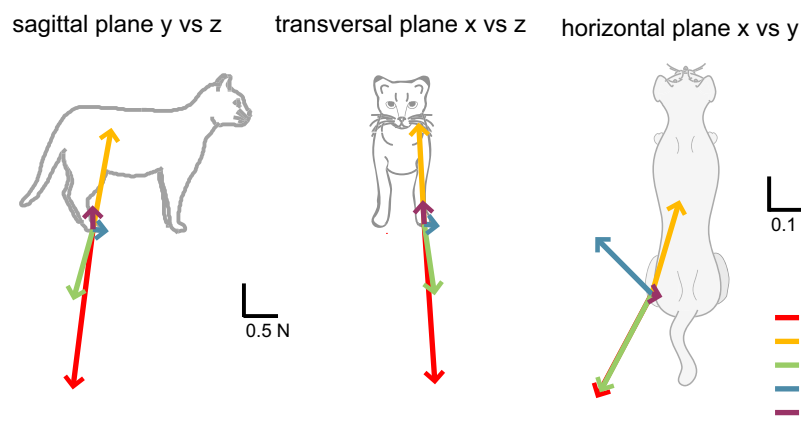## B Synergy Coefficients at different limb postures (C)

C Synergy Force Vectors (W_F)

FIG. 5. *A*: muscle synergy vectors, W_{EMG}, extracted from translation at the preferred stance distance for *cat Bi*. Each bar represents the relative level of activation for each muscle within the synergy (see Table 1 for muscle abbreviations). *B*: activation coefficients, C_i, for each of the 5 synergies at 4 stance distances. *Top traces* show background, quiet stance activation levels across direction. *Bottom traces* show the response to translation across direction. *C*: synergy force vectors, W_F, associated with each muscle synergy (same color coding), drawn in the sagittal, frontal, and horizontal planes. Vectors are expressed as forces applied by the limb against the support. Note that the scale for the horizontal plane has been magnified for easier viewing.

nent, which corresponds with the respective antigravity and flexor functions of the associated muscle synergies. W_{F3} produced a downward and posterior force relative to the limb axis that was similar to the quiet stance support vector, W_{F1}, at the preferred and long distances but less so at the shorter distances. W_{F4} produced an anterior force related to the anterior biarticular muscles, rectus femoris and anterior sartorius of W_4. Finally, W_{F5} produced an upward and medial force relative to the limb axis, consistent with the presence in W_5 of muscles with knee flexor action and the hip extensor/adductor, gracilis.

The synergy force vectors were able to account for the active forces during the postural response at all stance distances provided the ground reaction forces were rotated according to the angle of the background force during quiet standing, as illustrated in Fig. 7C by the reconstruction of each force component across stance distance. The shapes of the tuning curves were well reconstructed in most cases ($r^2 > 0.7$ in 81.8% of all force tuning curves in all cats at all stance distances). As stance distance decreased, the F-frame referenced anterior-posterior forces (Fy) increased in magnitude
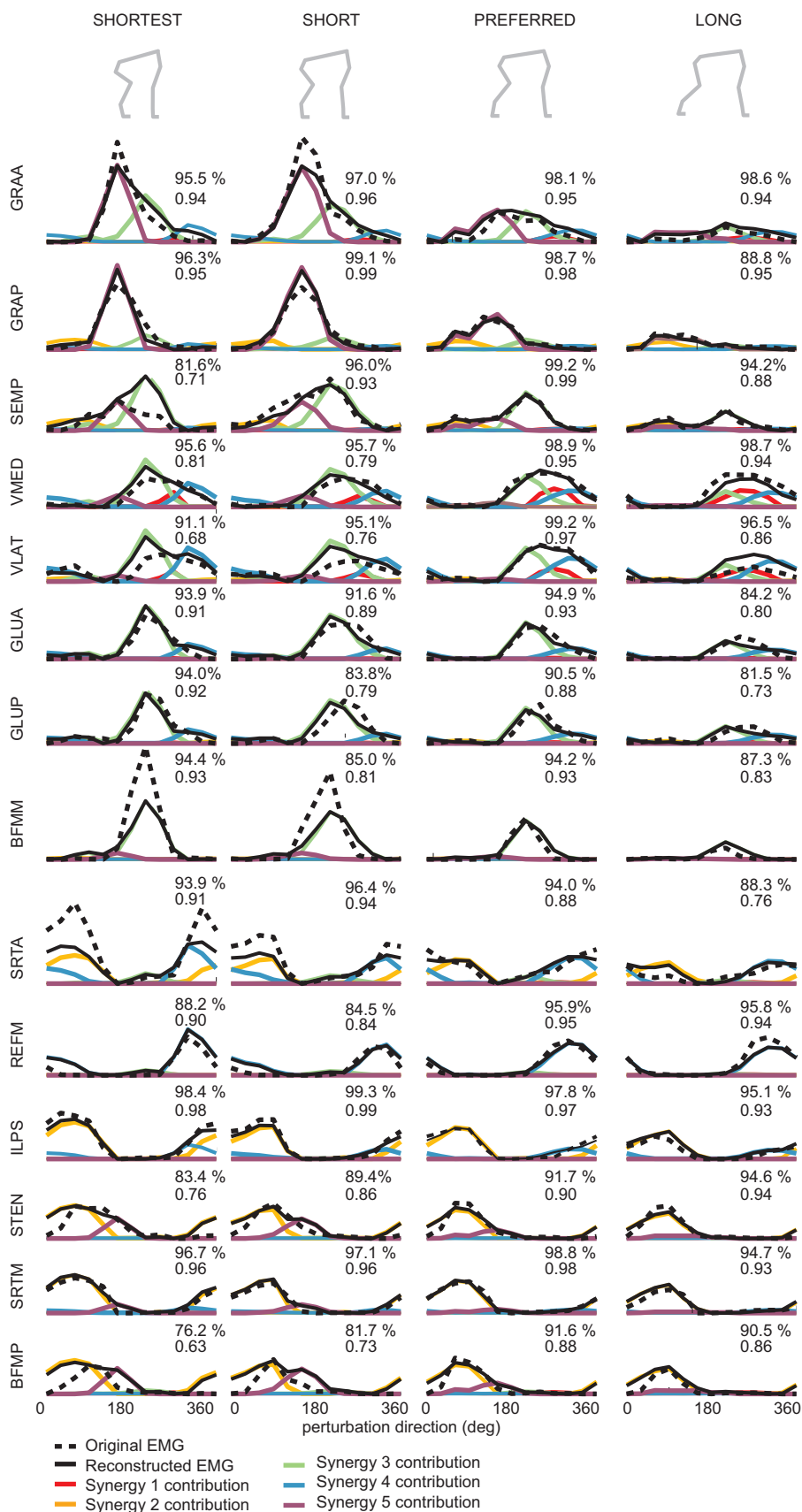
FIG. 6. EMG tuning curves of the automatic postural response in *cat Bi* for translations at 4 stance distances. - - -, original data; —, reconstructed data. The contribution from each synergy to the reconstruction is shown by the corresponding colored line. This is computed by multiplying each functional synergy vector *W* by its activation coefficient *C*.
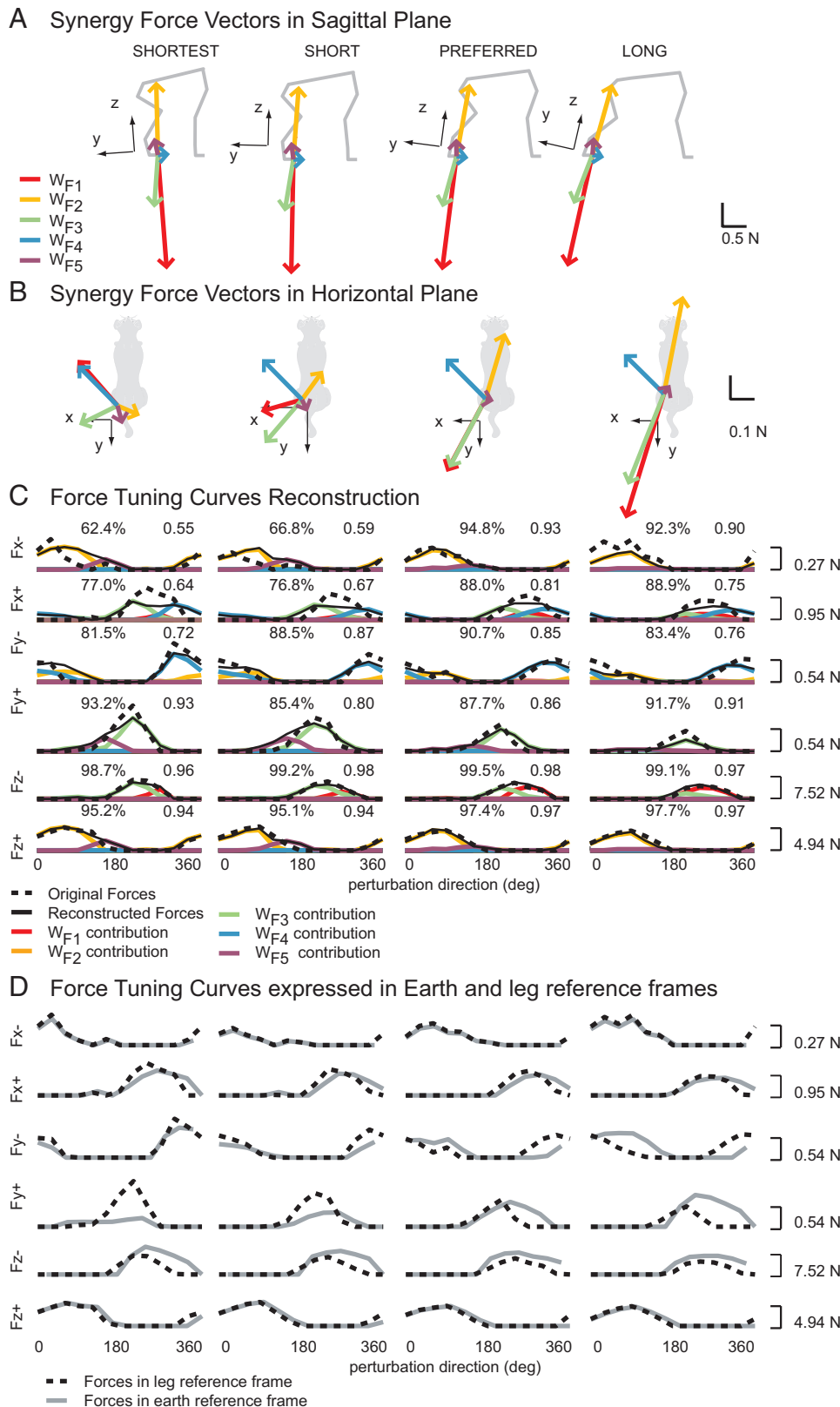
A Synergy Force Vectors in Sagittal Plane

B Synergy Force Vectors in Horizontal Plane

C Force Tuning Curves Reconstruction

- - - - Original Forces
——— Reconstructed Forces
——— W_{F1} contribution
——— W_{F2} contribution
——— W_{F3} contribution
——— W_{F4} contribution
——— W_{F5} contribution

D Force Tuning Curves expressed in Earth and leg reference frames

- - - - Forces in leg reference frame
——— Forces in earth reference frame

FIG. 7. *A* and *B*: synergy force vectors extracted from translation data at the preferred stance distance, for *cat Bi*. Vectors are expressed as forces applied by the limb against the support and are rotated in the sagittal plane such that the *z* axis is collinear with the mean GRF vector observed during quiet standing, which itself rotates with stance distance. Coordinate axes of the F-frame are shown at each stance distance. *C*: applied force tuning curves for translation at 4 stance distances for *cat Bi*, expressed in the F-frame coordinate system. Dashed line, original experimental data; solid line, reconstructed data; colored lines, contributions from each synergy force vector. *D*: tuning curves of the recorded force amplitude data from *cat Bi* for 4 stance distances. The forces have been separated into components as described in the text. The same data are drawn in 2 different coordinate reference frames, Earth-based (solid gray lines) and F-frame-based (dashed black lines). Note that the phase of the Fy force tuning curves remains constant when expressed in limb coordinates, but changes in Earth coordinates.

whereas the dorso-ventral (Fz) and lateral (Fx) forces were relatively consistent (Fig. 7*C*, original force traces). At short stances, the limb is protracted and the Fy⁺ component contributes to weight support (see coordinate frame for the short distance in Fig. 7*A*), which accounts for the change in amplitude with stance distance. These force changes parallel the increased magnitude in many of the EMGs at short compared with long stances.

TABLE 3. *Mean angle of GRF rotation, θ, for all cats at all stance distances*

Cat	Shortest	Short	Preferred	Long
Bi	−4.1	1.4	7.5	12.9
Ru	−4.5	0.35	6.9	18.5
Ni	−3.3	1	7	NA

GRF, ground reaction forces.

Synergies extracted from translation data can reconstruct rotation responses

In a separate set of cats, functional muscle synergies extracted from translations could be used to successfully reproduce EMG and force responses during rotation perturbations. The representative data of *cat Wo* are presented. Activation coefficients of the functional muscle synergies were different in rotation and translation across direction. The tuning curves of synergies W_1 and W_2 were the most similar, exhibiting only a small phase difference (Fig. 8). The activity level of synergies W_2, W_4, and W_5, which were dominated by biarticular muscles with a flexion moment arm at the hip or knee such as

sartorius, semitendinosus and rectus femoris, were effectively lower in rotations, consistent with the fact that many flexor muscle are not activated in response to rotations (Ting and Macpherson 2004). The direction of peak activation in W_3 was similar to translation, but the tuning curves for rotation were wider and flatter, and overall lower in amplitude. Finally, there was higher background activity in W_4 and W_5 compared with translation, suggesting that cats had a slightly different strategy for standing on the rotating platform.

The total mean VAF across all three cats was $>98.9 \pm 0.07$ and $>86.6 \pm 7.29\%$ for translations and rotations, respectively. The muscle synergies extracted from the translation data accounted well for most of the EMG tuning curves for rotation, which differed significantly in shape and amplitude from those evoked by translation in the identical muscles (Table 4 and Fig. 9A). Because some of the muscles had a relatively flat tuning curve where a high level of activation was present for all perturbation directions, r^2 was not always a good measure of the reconstruction fit. The criterion of VAF $>80\%$ provided a better assessment of degree of reconstruction of the original data (e.g., LGAS and TIBA in Fig. 9). In all the cats, the EMG tuning curve reconstructions matched the original data with
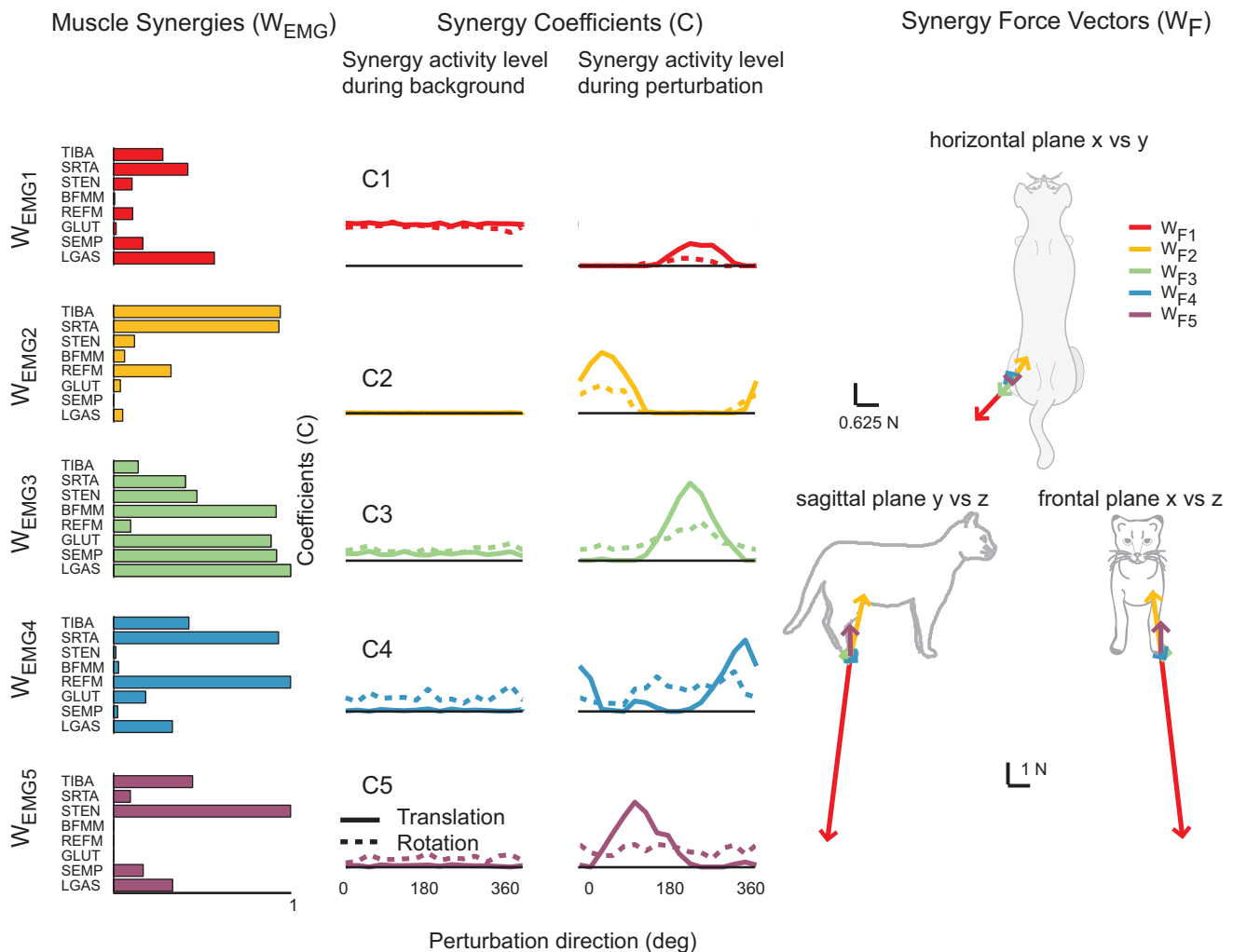

FIG. 8. Translation synergies applied to platform rotation data. *Left*: synergy vectors, *W*, extracted from translation data of *cat Wo*. *Middle*: activation coefficients, *C,* of each synergy for background activity during quiet stance and for the response to translation (—) and rotation (- - -). *Right*: synergy force vectors associated with each of the 5 muscle synergies, drawn in 3 planes.

TABLE 4. *r^2 or VAF values of EMG and force tuning curve reconstructions in translation-rotation group*

	Summary of EMG Reconstruction						Summary of Force reconstruction					
	VAF translation			VAF rotation			r^2 Translation			r^2 Rotation		
Cat	Minimum	Maximum	Average	Minimum	Maximum	Average	Minimum	Maximum	Average	Minimum	Maximum	Average
Kn	95.6	99.8	98.7	87.6	99.9	95.8	0.94	1.00	0.97	0.73	0.99	0.89
Wo	96.7	99.5	98.7	90.3	99.2	95.6	0.95	0.98	0.97	0.88	0.99	0.96
An	93.7	99.8	98.6	84.3	99.9	96.7	0.73	0.97	0.92	0.73	0.92	0.84

VAF >90% in 91% of muscle tuning curves (in all the muscles of *Wo*). Force tuning curves for rotation were well reconstructed using the synergy force vectors extracted from the control condition, with $r^2 > 0.9$ in 75% of all force tuning curves in all the cats (Table 4; $r^2 > 0.88$ for all force tuning curves of *Wo*; Fig. 9*B*).

Muscle synergies and synergy force vectors are consistent across cats

In all cats, the same number (5) of functional muscle synergies could reproduce the postural responses during all experimental conditions, and synergy composition, recruitment, and output were similar across cats (Fig. 10). Some differences in muscle synergy vectors and their activation coefficients across cats were found; nevertheless, all cats seem to follow the same postural control and biomechanical simplification strategy.

In the stance distance group, the muscle synergy vectors were similar across cats (Fig. 10*A*; $r^2 > 0.6$) except for W_{EMG3}, which had low correlation across cats, and W_{EMG1} of *Ni*, which had a low correlation when compared with the corresponding synergy of *Bi* ($r^2 = 0.47$). Nevertheless, the corresponding muscle synergies were activated for the same range of perturbation directions ($r^2 > 0.83$), except for C_5 of *Ni*, which was slightly phase-shifted relative to the other two cats (correlations $0.48 < r^2 < 0.54$). The synergy force vectors of *Bi* had similar directions to the corresponding synergy force vectors of the other two cats ($r^2 > 0.74$) except for W_{F3}, when compared with *Ru*, and W_{F5}, when compared with *Ni* (Fig. 10*A*). *Ru*'s synergy force vectors were similar to the corresponding syn-
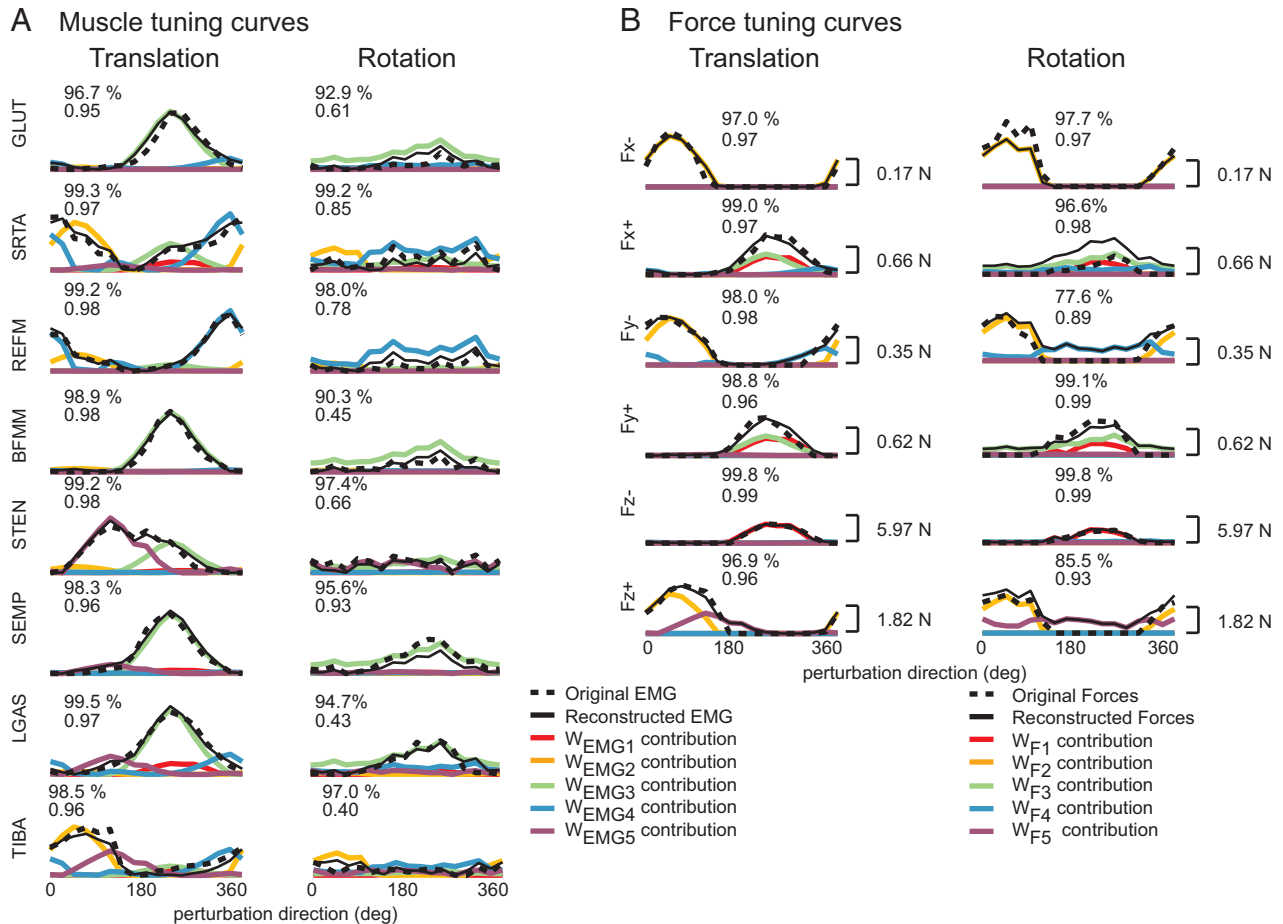

FIG. 9. Muscle (*A*) and force (*B*) tuning curves of the automatic postural response to translations (*left*) and rotations (*right*). Details as in Fig. 7. Force tuning curves are expressed in the Earth reference frame because cats stood at their preferred stance distance during both types of perturbation.
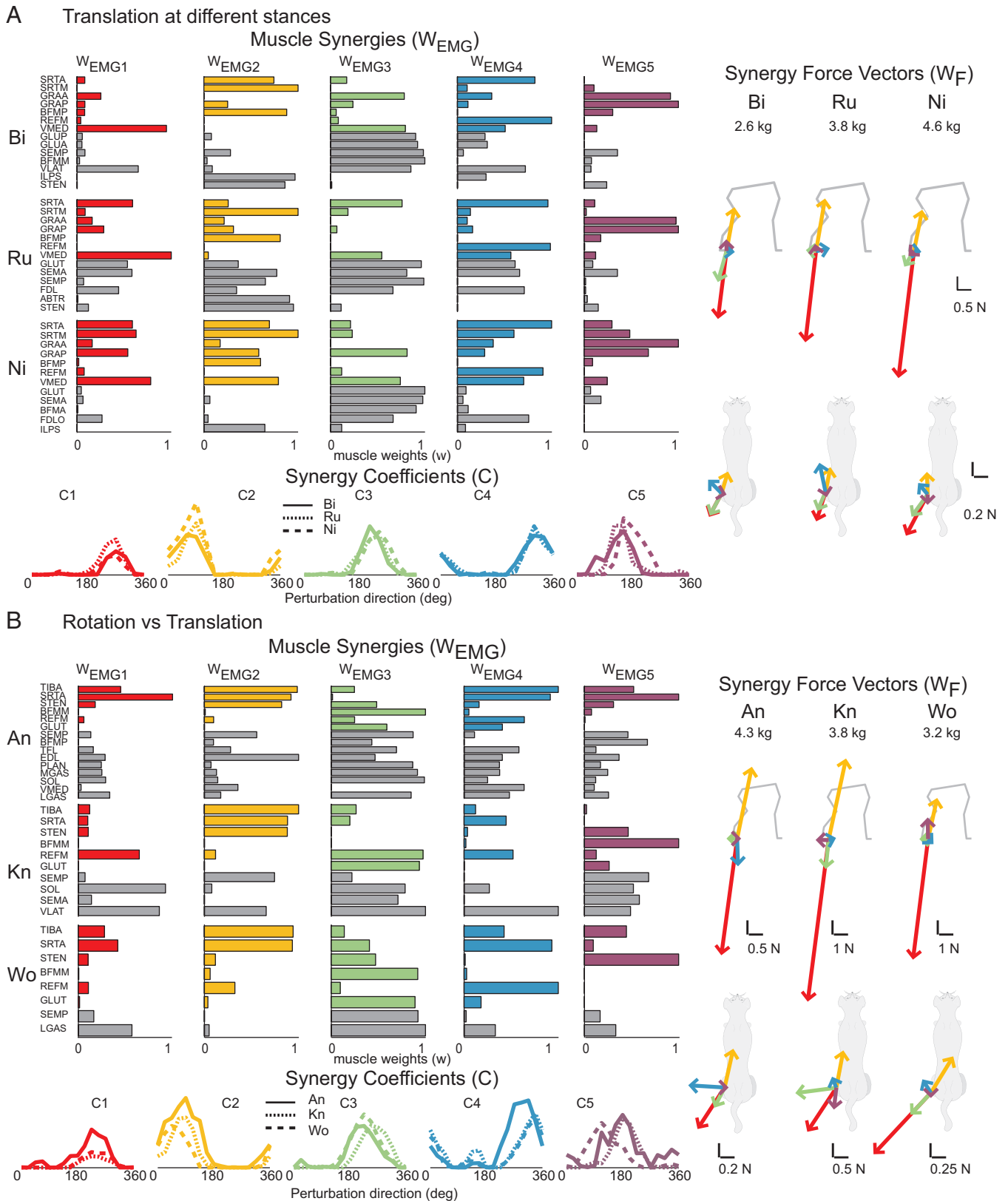
FIG. 10. Functional muscle synergies, synergy activation coefficients, and synergy force vectors across subjects. In all cats, 5 synergies accounted for >96% of the variability in response to translation at the preferred stance. The directional tuning of muscle synergy coefficients is similar across the 6 cats ($r^2 > 0.6$ except for C_5 of cats Ni and An). Muscle synergies are similar across cats ($r^2 > 0.6$) except for W_{EMG3} of the 6 cats and W_{EMG1} of cats Ni and Kn ($r^2 < 0.47$). The direction of three synergy force vectors, W_{F1} (red), W_{F2} (yellow), and W_{F4} (blue) is similar across cats ($r^2 > 0.74$) with the exception of W_{F4} of cats Ru and Kn (when compared with Ni). W_{F3} (green) and W_{F5} (purple) are only similar in some cases. Only those muscles recorded in common (indicated by colored bars) were used for calculating r^2 in the comparison of muscle synergies across cats. Gray bars indicate the remainder of muscles recorded in each subject.

ergy force vectors of the other cats except for W_{F3} ($r^2 < 0.48$) and both W_{F5} and W_{F4} when compared with the corresponding W_F's of Ni ($r^2 < 0.52$). In all the cats, the endpoint forces specified by each synergy were consistent across stance distance when rotated to the F-frame coordinate system.

Likewise in the translation-rotation group (Fig. 10B), all five muscle synergy vectors were similar across cats (Fig. 10A; $r^2 > 0.67$) except for W_{EMG3}, which had low correlation across cats, and W_{EMG1} of Kn, which had a low correlation when compared with the corresponding synergy of the other two cats. In all cats, the comparable muscle synergies were activated for the same range of perturbation directions ($r^2 > 0.6$) with the exception of the tuning coefficient C_5 ($r^2 < 0.58$) of An when compared with the corresponding coefficients of the other two cats. The synergy force vectors were very similar for two cats, An and Wo ($r^2 > 0.92$) with the exception of W_{F4} and W_{F5} ($r^2 < 0.58$). Kn's synergy force vectors differed somewhat from those of the other two cats ($r^2 < 0.34$) except for W_{F1} ($r^2 > 0.99$) and W_{F2} ($r^2 > 0.99$).

DISCUSSION

Our results show first that muscle synergy structure is robust across a variety of postural tasks and second that postural synergies generalize across subjects. Thus we conclude that muscle synergies and their related force vectors reflect a global control mechanism rather than an arbitrary outcome of the analysis technique. We will first discuss the validity of our methods, followed by the physiological significance in terms of a general scheme for the neural control of balance.

Methodological considerations

We believe that the basic characteristics of our five functional muscle synergies would emerge independent of the method of factorization or data analysis. Recent studies have demonstrated that many different factorization algorithms such as factor analysis (FA), independent components analysis (ICA), and NMF all produce similar results in terms of dimensional reduction and basic muscle synergy structure (Ivanenko et al. 2005; Tresch et al. 2006)

The number and characteristics of the functional synergies revealed in our NMF analysis was determined by the EMG patterns and not the force data, lending confidence to the conclusion that these synergies represent a basic organizational principle of neural control. Co-extraction of force with EMG was driven by our primary interest in identifying the set of synergy force vectors that is most closely related to the muscle synergies with the underlying assumption that muscle synergies reflect the output structure of the neural control system and produce task-related biomechanical effects (forces at the ground). Five synergies were required to reconstruct the data, whether EMG data were tested alone or in combination with the forces, whereas inclusion of forces in the dataset had little effect on muscle synergy composition.

Although EMG data are inherently positive and reflect the unidirectional nature of force generation by a muscle, GRF components may have positive and negative values. The challenge was to represent the force responses in a way that is physiologically relevant. We chose to separate the force APRs into six components composed of the absolute value of positive

and negative change from background, consistent with our previously published synergy studies (Jacobs and Macpherson 1996; Macpherson 1988a,b; Ting and Macpherson 2005). This approach obeys the nonnegative constraint of the NMF technique and resulted in physiologically meaningful synergy force vectors. For example, our previous studies showed that the limb unloading during translation is mediated by active flexion. By partitioning the forces into positive and negative changes, the activity of the flexor synergy can be represented as a flexor force at the endpoint of the limb. Moreover, our results distinguish this flexor activation from the decrease in the extensor activity producing antigravity support, which has a different synergy tuning curve that is not merely the inverse of the flexor one.

In theory, many different sets of force vectors could be found to adequately reconstruct the force space, but it would be difficult to determine the physiological significance of any particular force set in terms of neural output. We encountered this issue in our previous study in which force data were analyzed independent from EMG (Ting and Macpherson 2005). Some of the resultant force vectors did not correlate well with muscle synergy activation, leading us to speculate that such forces arose from other sources such as forces generated by a different limb.

It is possible that the reconstruction of the forces using NMF is not unique and a different set of synergy force vectors might be found with a different algorithm. However, muscle synergy characteristics were not affected by presence or absence of forces in the NMF analysis, and we obtain a consistent set of force vectors from the analysis. These results demonstrate that the set of force vectors that was extracted can reproduce the variations in the force data when the vector amplitudes are modulated exactly as the muscle synergies. Therefore we believe that the extracted forces reflect a plausible biomechanical function of each synergy.

A shortcoming of segmenting the forces is the possibility of underestimating the VAF in reconstruction of the *net* force. For example, during translation at 180° in long stance, the total F_x was close to zero (Fig. 7C). At this direction, synergies W_3 and W_5 were co-active such that W_3 (green trace) produced a small F_{x+} and W_5 (purple trace) produced a small F_{x-}. The summed effect was the correct net F_x of zero, but both F_{x+} and F_{x-} were overestimated, leading to a reduced VAF for both components. Fortunately, these effects were minimal in our data set but would need to be addressed for a data set containing more co-activation of muscle synergies. We did not find any muscle synergies that represented only co-contraction and that would have produced no net force, although antagonistic muscle activity was represented in each of the muscle synergies. Thus co-contraction independent of force production was not found.

We acknowledge that combining changes in force with total EMG in the APR portion of the dataset may introduce some small uncertainty in the parsing of EMG and force contributions between the quiet stance synergy (W_1) and the extensor synergy (W_3). However, by analyzing the total EMG during the background and during the postural response, we demonstrated that the response to translations includes not only the activation of various synergies but also the shutting down of the quiet stance synergy, W_1; this would not have emerged if we had analyzed the *change* in EMG. Therefore the errors that may have been introduced to accommodate the algorithm were

minimal and far outweighed the physiological interpretations we gained from using NMF. Nonlinearities in the negative and positive changes in force and EMG are inherent in the musculoskeletal physiology and, without a mechanistic model of EMG to force generation, may be difficult to handle mathematically, whatever algorithm is used.

Functional significance of synergies

Our data show that five synergies are sufficient to account for a wide variety of EMG and force patterns associated with changing task demands, in this case, due to changes in limb configuration or to changes in perturbation type. Variation in EMG and force was accomplished by modifying either the activation levels of synergies (altered stance distance) or the shape of their tuning curves (changing perturbation type). Some tasks may not require the full set of synergies (e.g., rotation used 4 synergies). Similarly, it has been shown that new synergies can arise when postural task mechanics change in humans (Krishnamoorthy et al. 2004) or in different types of locomotor tasks in frogs (D'Avella and Bizzi 2005).

By including the background muscle activity in our analysis, we were able to identify two muscle synergies that were associated with similar extensor force vectors yet had different roles for balance control and could represent differences in muscle synergy composition at the motor-unit level. Our analysis revealed an explicit representation of an extensor synergy (W_1) that not only assumes the primary role for antigravity weight support during quiet stance but also drops out during the dynamic postural response even when the limb is loaded. The second extensor synergy (W_3) recruits several muscles in common with W_1 and generates a similar force, but it is recruited during the postural response and not during quiet stance. It is possible that the two extensor synergies activate different sets of motor units within a given muscle with slow twitch units for quiet standing and faster twitch units for the rapid response to perturbation. Analysis at the single motor-unit level is required to test this idea. Nevertheless, the separation of weight support and of the dynamic response to perturbation into two separate synergies suggests some level of independence in the neural control of these two functions, as previously suggested from our study of postural responses in the spinally transected cat (Macpherson and Fung 1999).

There was evidence of nonlinear recruitment of individual muscles within a synergy as a function of stance distance. This was evident in biarticular thigh muscles where the correct spatial pattern but an incorrect magnitude was predicted. For example, BFMM was activated more than predicted for long stance and less than predicted for short stance (Fig. 6). One explanation concerns the change in muscle length with change in limb orientation that accompanies variations in stance distance. Some muscles, particularly those crossing more than one joint, may be significantly shortened or lengthened at the extremes of stance distance, such that the relationship between EMG and force is no longer within the linear range assumed by our analysis method. Another explanation is that under certain conditions, the relationship between the descending command to a muscle synergy and the magnitude of change in EMG could differ for various specific muscles within the synergy. This could occur due to the additional influence of position-dependent sensory feedback altering the excitability of individual muscles at different stance distances. For example, static joint angle changes can alter H-reflex and stretch reflex gains in humans (Knikou and Rymer 2002, 2003; Stein and Kearney 1995), and muscle activation amplitude in response to direct spinal cord stimulation in the cat (Lemay and Grill 2004).

Functional consequences of limb-referenced synergy force vectors

Our previous studies of the postural response to translation described variations in the force constraint strategy with stance distance (Macpherson 1994) that we believe can now be explained in terms of functional muscle synergies and their relationship to limb-referenced force vectors. The force constraint strategy (Macpherson 1988a) refers to the forces produced by a single limb during multi-directional postural perturbations, which are constrained to act along a diagonal axis directed roughly toward and away from the CoM. At long stance distances, this alignment is augmented, and at short stance distances, the force directions are more evenly distributed (Macpherson 1994). It has not been clear whether the source of this constraint is neural or mechanical. The use of a force directed toward the CoM appears to be advantageous for coordinating forces across many limbs, to provide stability and minimize torques at individual joints, as well as those that rotate the body (Full et al. 1991). Therefore at the preferred stance distance, the most useful muscle synergies would be those directed roughly along this stabilizing axis. However, because the same muscle synergies are used at all postures, the contributions of the synergy force vectors in the horizontal plane change as the limb rotates. At long stance distances, four of five synergy force vectors are aligned along the diagonal axis in the Earth-based horizontal plane (Fig. 7B), leaving few options for generating forces in other directions. At short stance distances, the synergy force vectors rotate away from the diagonal axis and have projections in many directions, which can account for the relaxation of the force constraint. Therefore the change in the force constraint strategy with stance distance is an emergent property which arises naturally from a neural strategy of using the same functional muscle synergies at all stance distances. The endpoint force generated depends on the production of synergy force vectors that are consistent within the limb reference frame, but are used to stabilize the CoM in the extrinsic reference frame.

Expressing the synergy force vectors in limb axis coordinates also explains the decrease of EMG activity in many muscles as well as the decrease in synergy coefficients, *C,* with increase in stance distance. The longer the stance distance, the larger are the horizontal plane force components of the synergy force vectors along the antero-medial to postero-lateral axis (primarily W_1, W_3, and W_5). Thus correspondingly less activation of these functional muscle synergies is required to generate the same horizontal force magnitude in the limb for long compared with short stance distances. Furthermore, at short stance distances, W_3 (green) and W_5 (purple), which contain many of the posterior thigh muscles, must be activated to achieve a net force in the posterior and downward direction. However, the component of these synergy forces in the posterior direction is quite small; therefore a relatively higher activation level is required, to generate an adequate horizontal

force. Similarly, in human postural responses, muscle activity is reduced when stance width is increased (Henry et al. 2001).

How are synergies encoded in the nervous system?

The robustness of the set of five synergies suggests that this output organization does not arise from reflex pathways nor from biomechanically imposed constraints. The various types of postural perturbations examined in the current study evoked widely differing sensory input signals, even when the disturbance propelled the body center of mass in the same direction. A good example is rotation and translation that evoked similar EMG_{APR}s, yet caused widely different patterns of sensory inputs in muscle spindles, Golgi tendon organs, and vestibular organs due to the opposite mechanical effects on muscle length, joint angle change, and head acceleration (Nashner 1976; Ting and Macpherson 2004). The commonality between rotation and translation perturbations that elicit similar postural responses is the CoM kinematics with respect to the feet, which is probably represented in the nervous system as a derived variable based on multisensory integration of cutaneous and other inputs from many body regions (Ting and Macpherson 2004). Thus it is unlikely that functional muscle synergies are simply a reflexive response due to a particular set of sensory inputs but rather that they represent a central mechanism for coordination of motor outputs.

Muscle synergies provide a modular control mechanism whereby higher neural control centers need only specify the desired task-level function such as force at the ground, and not the detailed coordination of muscles across multiple joints. This scheme could include the activation of spinal synergies through simple higher-level commands, as has been suggested from locomotor studies (Hart and Giszter 2004; Saltiel et al. 2001, 2005). More generally, one might predict the existence of neuronal networks or populations that specify the synergy activation patterns (C), and the outputs of which are distributed (perhaps multisynaptically) to the motoneurons of muscles within the synergy. The consistency of synergy activation and force vectors across individuals suggests that a neural organization encoding low-dimensional variables is a basic component of the motor-control system. However, the variation in muscle synergy composition (W_{EMG}) across subjects suggests a flexibility of expression within the set of equivalent solutions present in a redundant musculoskeletal system. Because each individual has a stable muscle synergy composition across postural condition and days, the particular composition of muscle synergies may be tuned to the body morphology and mechanics of each individual but modifiable through learning and experience.

In the context of postural control, muscle synergies are likely to be coordinated in supraspinal structures such as brain stem or cerebellum because of the need to integrate multimodal sensory inputs from somatosensory, visual, and vestibular sources. Postural responses to translation are notably absent in the hindlimbs of cats with spinal cord transection at the T_6 level (Macpherson and Fung 1999), yet weight support for quiet standing can still be achieved (Edgerton et al. 2001; Macpherson and Fung 1999). Perhaps the extensor synergy (W_1), or some vestige of it, can be accessed in the isolated spinal cord, whereas the other synergies require connectivity to higher centers. The horizontal plane force components of the extensor synergy for quiet stance may account for the ability of the spinal cat to withstand small perturbations, by virtue of the stiffness of the activated muscles and the resultant force vector along the diagonal axis. Therefore muscle synergies encoded in the spinal cord (Giszter et al. 1993; Lemay and Grill 2004; Saltiel et al. 2001) may not play a role in directional balance control. Reticulospinal neurons branch to innervate many different spinal levels and could send synergy commands to many muscles spanning multiple joints (Matsuyama et al. 2004). Or synergies may be accessed from a variety of neuronal networks, which could account for differences in their modulation and changes with neurological impairments. Evidence from stroke and spinal cord patients during locomotion also suggest that higher centers may be necessary for appropriate synergies to arise (Bourbonnais et al. 1989; Brown et al. 1997; Ivanenko et al. 2003).

The organization of motor outputs according to task-level variables provides a parsimonious symmetry with the integration of sensory inputs in the nervous system. In a feedback control loop, the sensory information would first be transformed into task-level variables, for example, CoM displacement and velocity, which would then cause a functional muscle synergy to be activated. Such an organization is consistent with the fact that structures throughout the nervous system appear to integrate both sensory inputs (Bosco and Poppele 1997; Poppele et al. 2002), and motor commands (Georgopoulos et al. 1986, 1992) to reflect task-level variables. Specifically, limb axis orientation is encoded by ascending neurons in the dorsospinal-cerebellar tract (DSCT) and is therefore a readily available derived variable (Bosco and Poppele 1997; Bosco et al. 1996) that has been hypothesized to be an important task-level variable for the neural control of stance in the cat (Lacquaniti and Maioli 1994). Such information would be necessary to activate functional muscle synergies that are encoded in a limb-axis reference frame.

In conclusion, we identified a set of five functional muscle synergies that was robust across a range of dynamic postural tasks as well as quiet stance and generalized across subjects. This finding suggests that a synergy organization forms part of the neural control structure for the motor system. This type of neural mechanism effectively reduces the musculoskeletal redundancy inherent in the multisegmented limb and allows for rapid activation of functionally appropriate responses for automatic postural adjustments. It is likely that such a control structure underlies other types of automatic as well as voluntary movements. Similar sharing of motor output units has been demonstrated in rhythmic tasks such as paw shake and locomotion (Baev et al. 1991; Carter and Smith 1986a,b; Stein 2005). The identification of functional muscle synergies may provide a means for understanding the task-level variables that are used by the nervous system to encode sensory inputs as well as motor outputs (d'Avella and Bizzi 2005; Poggio and Bizzi 2004).

REFERENCES

Alizadeh AA, Eisen MB, Davis RE, Ma C, Lossos IS, Rosenwald A, Boldrick JC, Sabet H, Tran T, Yu X, Powell JI, Yang L, Marti GE, Moore T, Hudson J, Jr, Lu L, Lewis DB, Tibshirani R, Sherlock G, Chan WC, Greiner TC, Weisenburger DD, Armitage JO, Warnke R, Levy R, Wilson W, Grever MR, Byrd JC, Botstein D, Brown PO, and Staudt LM. Distinct types of diffuse large B-cell lymphoma identified by gene expression profiling. *Nature* 403: 503–511, 2000.

Baev KV, Esipenko VB, and Shimansky YP. Afferent control of central pattern generators—experimental-analysis of locomotion in the decerebrate cat. *Neuroscience* 43: 237–247, 1991.

Bosco G and Poppele RE. Representation of multiple kinematic parameters of the cat hindlimb in spinocerebellar activity. *J Neurophysiol* 78: 1421–1432, 1997.

Bosco G, Rankin A, and Poppele R. Representation of passive hindlimb postures in cat spinocerebellar activity. *J Neurophysiol* 76: 715–726, 1996.

Bourbonnais D, Vandennoven S, Carey KM, and Rymer WZ. Abnormal spatial patterns of elbow muscle activation in hemiparetic human-subjects. *Brain* 112: 85–102, 1989.

Brown DA, Kautz SA, and Dairaghi CA. Muscle activity adapts to anti-gravity posture during pedalling in persons with post-stroke hemiplegia. *Brain* 120: 825–837, 1997.

Carter MC and Smith JL. Simultaneous control of 2 rhythmical behaviors. I. Locomotion with paw-shake response in normal cat. *J Neurophysiol* 56: 171–183, 1986a.

Carter MC and Smith JL. Simultaneous control of 2 rhythmical behaviors. II. Hindlimb walking with paw-shake response in spinal cat. *J Neurophysiol* 56: 184–195, 1986b.

d'Avella A and Bizzi E. Shared and specific muscle synergies in natural motor behaviors. *Proc Natl Acad Sci USA* 102: 3076–3081, 2005.

d'Avella A, Saltiel P, and Bizzi E. Combinations of muscle synergies in the construction of a natural motor behavior. *Nat Neurosci* 6: 300–308, 2003.

Edgerton VR, Leon RD, Harkema SJ, Hodgson JA, London N, Reinkensmeyer DJ, Roy RR, Talmadge RJ, Tillakaratne NJ, Timoszyk W, and Tobin A. Retraining the injured spinal cord. *J Physiol* 533: 15–22, 2001.

Eisen MB, Spellman PT, Brown PO, and Botstein D. Cluster analysis and display of genome-wide expression patterns. *Proc Natl Acad Sci USA* 95: 14863–14868, 1998.

Full RJ, Blickhan R, and Ting LH. Leg design in hexapedal runners. *J Exp Biol* 158: 369–390, 1991.

Fung J and Macpherson JM. Determinants of postural orientation in quadrupedal stance. *J Neurosci* 15: 1121–1131, 1995.

Fung J and Macpherson JM. Attributes of quiet stance in the chronic spinal cat. *J Neurophysiol* 82: 3056–3065, 1999.

Georgopoulos AP, Ashe J, Smyrnis N, and Taira M. The motor cortex and the coding of force. *Science* 256: 1692–1695, 1992.

Georgopoulos AP, Schwartz AB, and Kettner RE. Neuronal population coding of movement direction. *Science* 233: 1416–1419, 1986.

Giszter SF, Mussa-Ivaldi FA, and Bizzi E. Convergent force fields organized in the frog's spinal cord. *J Neurosci* 13: 467–491, 1993.

Hart CB and Giszter SF. Modular premotor drives and unit bursts as primitives for frog motor behaviors. *J Neurosci* 24: 5269–5282, 2004.

Henry SM, Fung J, and Horak FB. Effect of stance width on multidirectional postural responses. *J Neurophysiol* 85: 559–570, 2001.

Ivanenko YP, Cappellini G, Dominici N, Poppele RE, and Lacquaniti F. Coordination of locomotion with voluntary movements in humans. *J Neurosci* 25: 7238–7253, 2005.

Ivanenko YP, Grasso R, Zago M, Molinari M, Scivoletto G, Castellano V, Macellari V and Lacquaniti F. Temporal components of the motor patterns expressed by the human spinal cord reflect foot kinematics. *J Neurophysiol* 90: 3555–3565, 2003.

Ivanenko YP, Poppele RE, and Lacquaniti E. Five basic muscle activation patterns account for muscle activity during human locomotion. *J Physiol* 556: 267–282, 2004.

Jacobs R and Macpherson JM. Two functional muscle groupings during postural equilibrium tasks in standing cats. *J Neurophysiol* 76: 2402–2411, 1996.

Knikou M and Rymer Z. Effects of changes in hip joint angle on H-reflex excitability in humans. *Exp Brain Res* 143: 149–159, 2002.

Knikou M and Rymer WZ. Static and dynamic changes in body orientation modulate spinal reflex excitability in humans. *Exp Brain Res* 152: 466–475, 2003.

Krishnamoorthy V, Latash ML, Scholz JP, and Zatsiorsky VM. Muscle synergies during shifts of the center of pressure by standing persons. *Exp Brain Res* 152: 281–292, 2003.

Krishnamoorthy V, Latash ML, Scholz JP, and Zatsiorsky VM. Muscle modes during shifts of the center of pressure by standing persons: effect of instability and additional support. *Exp Brain Res* 157: 18–31, 2004.

Lacquaniti F and Maioli C. Independent control of limb position and contact forces in cat posture. *J Neurophysiol* 72: 1476–1495, 1994.

Lee DD and Seung HS. Algorithms for non-negative matrix factorization. *Adv Neural Info Proc Syst* 13: 556–562, 2001.

Lemay MA and Grill WM. Modularity of motor output evoked by intraspinal microstimulation in cats. *J Neurophysiol* 91: 502–514, 2004.

Macpherson JM. Strategies that simplify the control of quadrupedal stance. I. Forces at the ground. *J Neurophysiol* 60: 204–217, 1988a.

Macpherson JM. Strategies that simplify the control of quadrupedal stance. II. Electromyographic activity. *J Neurophysiol* 60: 218–231, 1988b.

Macpherson JM. Changes in a postural strategy with inter-paw distance. *J Neurophysiol* 71: 931–940, 1994.

Macpherson JM and Fung J. Weight support and balance during perturbed stance in the chronic spinal cat. *J Neurophysiol* 82: 3066–3081, 1999.

Macpherson JM, Lywood DW, and Van Eyken A. A system for the analysis of posture and stance in quadrupeds. *J Neurosci Methods* 20: 73–82, 1987.

Matsuyama K, Mori F, Nakajima K, Drew T, Aoki M, and Mori S. Locomotor role of the corticoreticular-reticulospinal-spinal interneuronal system. *Prog Brain Res* 143: 239–249, 2004.

Nashner LM. Adapting reflexes controlling the human posture. *Exp Brain Res* 26: 59–72, 1976.

Poggio T and Bizzi E. Generalization in vision and motor control. *Nature* 431: 768–774, 2004.

Poppele R and Bosco G. Sophisticated spinal contributions to motor control. *Trends Neurosci* 26: 269–276, 2003.

Poppele RE, Bosco G, and Rankin AM. Independent representations of limb axis length and orientation in spinocerebellar response components. *J Neurophysiol* 87: 409–422, 2002.

Raasch CC and Zajac FE. Locomotor strategy for pedaling: muscle groups and biomechanical functions. *J Neurophysiol* 82: 515–525, 1999.

Raasch CC, Zajac FE, Ma B, and Levine WS. Muscle coordination of maximum-speed pedaling. *J Biomech* 30: 595–602, 1997.

Saltiel P, Wyler-Duda K, d'Avella A, Ajemian RJ, and Bizzi E. Localization and connectivity in spinal interneuronal networks: the adduction-caudal extension-flexion rhythm in the frog. *J Neurophysiol* 94: 2120–38, 2005.

Saltiel P, Wyler-Duda K, D'Avella A, Tresch MC, and Bizzi E. Muscle synergies encoded within the spinal cord: Evidence from focal intraspinal NMDA iontophoresis in the frog. *J Neurophysiol* 85: 605–619, 2001.

Stein P. Neuronal control of turtle hindlimb motor rhythms. *J Comp Physiol A Neuroethol Sens Neural Behav Physiol* 191: 213–229, 2005.

Stein RB and Kearney RE. Nonlinear behavior of muscle reflexes at the human ankle joint. *J Neurophysiol* 73: 65–72, 1995.

Ting LH, Kautz SA, Brown DA, and Zajac FE. Phase reversal of biomechanical functions and muscle activity in backward pedaling. *J Neurophysiol* 81: 544–551, 1999.

Ting LH, Kautz SA, Brown DA, and Zajac FE. Contralateral movement and extensor force generation alter flexion phase muscle coordination in pedaling. *J Neurophysiol* 83: 3351–3365, 2000.

Ting LH and Macpherson JM. Ratio of shear to load ground-reaction force may underlie the directional tuning of the automatic postural response to rotation and translation. *J Neurophysiol* 92: 808–823, 2004.

Ting LH and Macpherson JM. A limited set of muscle synergies for force control during a postural task. *J Neurophysiol* 93: 609–613, 2005.

Ting LH, Raasch CC, Brown DA, Kautz SA, and Zajac FE. Sensorimotor state of the contralateral leg affects ipsilateral muscle coordination of pedaling. *J Neurophysiol* 80: 1341–1351, 1998.

Tresch MC, Cheung VC, and d'Avella A. Matrix factorization algorithms for the identification of muscle synergies: evaluation on simulated and experimental data sets. *J Neurophysiol* 95: 2199–2212, 2006.

Tresch MC, Saltiel P, and Bizzi E. The construction of movement by the spinal cord. *Nat Neurosci* 2: 162–167, 1999.

Weiss EJ and Flanders M. Muscular and postural synergies of the human hand. *J Neurophysiol* 92: 523–535, 2004.

Zar JH. *Biostatistical Analysis.* Upper Saddle River, NJ: Prentice-Hall, 1999.